DIRECT EXTRACTION OF GaAs MESFET INTRINSIC ELEMENT AND PARASITIC INDUCTANCE VALUES

Eric Arnold, Michael Golio, Monte Miller, and Bill Beckwith

Motorola Inc., Strategic Electronics Division
Chandler, AZ 85248-2899

Abstract - **A simple method is described for extracting the intrinsic element and parasitic inductance values for the GaAs MESFET equivalent circuit. The intrinsic element values are extracted from low frequency y-parameter data de-embedded through previously determined parasitic resistances. Parasitic inductance values are then evaluated by comparing the resulting modeled z-parameters with the extrinsic measured z-parameters. All elements are extracted from the same set of hot FET S-parameter measurements. The method is very fast and the resulting equivalent circuit provides an excellent match to measured s-parameters through 18 GHz.**

I. INTRODUCTION

Tasks such as RF parameter monitoring of MMIC devices [1] and large-signal model generation [2], [3] require the reduction of a large number of s-parameter sets into an equivalent circuit format. Although numerical optimization techniques have often been used for extracting these small-signal models, their problems with uniqueness [4] and long execution times make them impractical here. Fast techniques for extracting complete small-signal models have been described previously [5], but all require the additional RF characterization of the cold FET in order to extract parasitic inductance. This is both inconvenient and potentially inaccurate, since the model has not been derived solely from the data it is asked to model. This is particularly true of MMIC devices where parasitic gate inductance is proportional to the depletion depth under the gate [6]. The method described here requires only RF characterization at the device operating point and knowledge of the parasitic resistances. In particular, we have employed the d.c. measurement technique described by Fukui [7] to determine these parasitic resistances. The technique has been successfully applied to discrete GaAs FETs, MMIC GaAs FETs and to HEMTs.

Section II of this paper describes the theory behind this technique and outlines a simple algorithm which can be used to obtain successively better approximations to the element values. In section III this method is applied to the element extraction of a Triquint 0.5μ by 300μ MMIC device. Section III also presents results obtained over a range of bias values with the Triquint device. The equivalent circuit derived by this method is shown to provide an excellent match to measured s-parameters throughout the measurement range with a typical modeling error of less than 5 %.

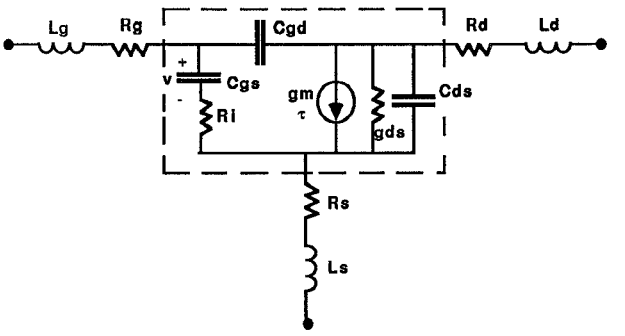

Fig. 1. Small-signal equivalent circuit of the GaAs FET to 18 GHz.

II. ANALYSIS

The FET equivalent circuit is shown in Figure 1. To begin the analysis it is assumed that the parasitic resistances have been measured. De-embedding through the parasitic elements, the intrinsic device z-parameters can be expressed as

$$z_{11} = Z_{11} - (R_g + R_s) - j\omega(L_g + L_s) \quad (1)$$

$$z_{12} = Z_{12} - R_s - j\omega L_s \quad (2)$$

$$z_{21} = Z_{21} - R_s - j\omega L_s \quad (3)$$

$$z_{22} = Z_{22} - (R_d + R_s) - j\omega(L_d + L_s), \quad (4)$$

where the extrinsic z-parameters are denoted by upper case letters and are easily obtained from the measured s-parameters using standard conversion formulas. At sufficiently low frequencies, $|\omega L| << |IM[Z_{ij}(\omega)]|$, and the inductances have a minimal effect on (1)-(4). The intrinsic z-parameters can then be computed in this low frequency range and converted to y-parameters. The intrinsic element values are then extracted from (5)-(8), [8] by plotting the real and imaginary parts of each y-parameter vs. frequency and performing a regression fit to this data. The expressions are valid for $(\omega C_{gs} R_i)^2 << 1$ and $\omega\tau << 1$.

$$y_{11} = R_i C_{gs}^2 \omega^2 + j\omega(C_{gs} + C_{gd}) \quad (5)$$

$$y_{12} = -j\omega C_{gd} \quad (6)$$

$$y_{21} = g_m - j\omega(C_{gd} + g_m(R_i C_{gs} + \tau)) \quad (7)$$

$$y_{22} = 1/R_{ds} + j\omega(C_{ds} + C_{gd}). \quad (8)$$

To a good approximation, any differences between the measured and modeled z-parameters at *high frequency* can be accounted for by the absence of inductances in the model. From (1)-(4) we obtain the following expressions for the parasitic inductances which are valid for $f > f_m$, where f_m is the maximum frequency used to evaluate the intrinsic element values:

$$IM[Z_{11}] - IM[z_{11mod}] = \Delta Z_{11} = \omega(L_g + L_s) \quad (9)$$

$$IM[Z_{12}] - IM[z_{12mod}] = \Delta Z_{12} = \omega L_s \quad (10)$$

$$IM[Z_{21}] - IM[z_{21mod}] = \Delta Z_{21} = \omega L_s \quad (11)$$

$$IM[Z_{22}] - IM[z_{22mod}] = \Delta Z_{22} = \omega(L_d + L_s). \quad (12)$$

The inductance values are then easily obtained from the ΔZ_{ij} data as follows:

1) L_s from ΔZ_{12} or ΔZ_{21}.

2) L_g from ΔZ_{11}.

3) L_d from ΔZ_{22}.

The value of L_s extracted can vary considerably depending on whether one uses ΔZ_{12} or ΔZ_{21} to find it. Since the determination of L_s by either method requires relatively simple calculations, in many cases it may be worthwhile to perform the calculation both ways and then determine which provides the least error. Alternatively, one can use a weighted average and compute L_s from

$$L_s = \frac{(W_{12}L_s^{12} + W_{21}L_s^{21})}{(W_{12} + W_{21})} \quad (13)$$

where W_{12} and W_{21} are the weighting factors and L_s^{12} and L_s^{21} are the inductances extracted from ΔZ_{12} or ΔZ_{21} respectively. The weighting factors can either be selected by trial and error or varied automatically in the extraction algorithm so as to obtain the desired tradeoff between the modeling errors in Z_{12} and Z_{21}.

Successively better approximations to both the intrinsic and extrinsic element values can be obtained by repeating this extraction procedure but de-embedding the inductance found in the previous iteration in all subsequent iterations. Diminishing returns in increased accuracy are usually achieved after 2 or 3 iterations. The algorithm is as follows:

1) Convert measured s-parameters to z-parameters.
2) Evaluate inductances from (9)-(12) (inductors set to 0 for first iteration).
3) De-embed parasitics to obtain low-frequency intrinsic z-parameters using (1)-(4)
4) Convert intrinsic z-matrix to a y-matrix.
5) Evaluate intrinsic elements from y-parameter data fit to eqs. (5)-(8).
6) Compute modeled z-parameters from circuit elements found in step 5.
7) Compute modeling error E_{mod}.
8) If $E_{mod} < E_{tol}$ then go to 9, otherwise go to 2.
9) Stop.

III. RESULTS

The algorithm described in section II has been coded into a computer program and has been used extensively for the small-signal characterization of both MMIC and discrete devices. The program is a subset of a complete in house developed package which permits 1) Automated measurement of d.c. parasitic resistances; 2) Automated s-parameter characterization vs. bias; 3) Small-signal model extraction and tabulation of element values vs. bias; 4) Extraction of large-signal model parameters for best fit to both d.c. and r.f. data [10].

In this section, we present results on the small-signal characterization of a Triquint 300μ by 0.5μ MMIC device. The parasitic resistances were first measured using an automated Fukui measurement. The values are R_g = 2.0 Ω, R_d = 3.6 Ω, R_s = 3.1 Ω. The device s-parameters were measured in a Cascade Microtech probe station with a HP-8720 network analyzer under computer control. The device was characterized from 1-18 GHz over the bias range V_{ds} = 0.5, 1.0, 1.5, 3.0, 5.0 V for each gate voltage V_{gs} = -1.8, -1.2, -0.8, -0.4, 0.0 V.

A. Intrinsic Element Extraction

Figure 2 shows the frequency dependence of the imaginary parts of y_{12}, y_{22}, and y_{11} for the Triquint device with the resistances de-embedded. The device was biased at V_{ds} = 3 V, V_{gs} = -0.8 V. Since this data is linear with frequency, the three equivalent circuit capacitances are easily extracted from the slopes of these plots per eqs. (5), (6), and (8). Both output conductance g_{ds} and transconductance g_m remain relatively constant in the low frequency (1 - 2.5 GHz) range and are evaluated by averaging $RE[y_{21}]$ and $RE[y_{22}]$ respectively over this frequency range. The intrinsic element values are shown in the first column of Table I along with the associated modeling errors. The modeling error was computed from 1 to 18 GHz with the expression

$$E_{ij} = \frac{1}{n}\sum_{k=1}^{n} \frac{|S_{ijmeas}^k - S_{ijmod}^k|}{|S_{ijmeas}^k|} \quad (14)$$

where n is the number of frequencies used in the analysis. For the examples presented here, 17 discrete frequencies were used (1- 18 GHz in increments of 1 GHz). The element values were computed without regard for the presence of any parasitic inductance. Hence, the values shown represent the results obtained after the first iteration of our algorithm.

Although a value for R_i can be extracted from a linear fit to $RE[y_{11}]$ vs. ω^2 data, this low frequency y_{11} data is often quite noisy which results in a very low correlation data fit and therefore, large uncertainty in R_i. We have found, that in many cases, the absence of R_i has minimal impact on the model's accuracy and can therefore be neglected. In addition, when one is solving the small-signal model as a precursor to large-signal model development, R_i is of no consequence since it is rarely included in the large-signal topology. If a value for R_i must be extracted, a more reliable method may be to optimize R_i to match S_{11} after the other elements have been computed [9].

A typical plot from which the transit time τ can be extracted is shown in Fig. 3. Although not as noisy as the R_i data, extraction of τ values by this method can be as much as 25 % in error. A more accurate determination of τ requires the use of higher frequency data, since the primary parameter τ effects is S_{21} at higher frequencies. Unfortunately, the simple expression which permits the direct determination of τ is only valid at low frequency.

B. Parasitic Inductance Extraction

The quantity ΔZ_{11} is plotted in Fig. 4 for the Triquint device using the column 1 data of Table I. The best weighting factors

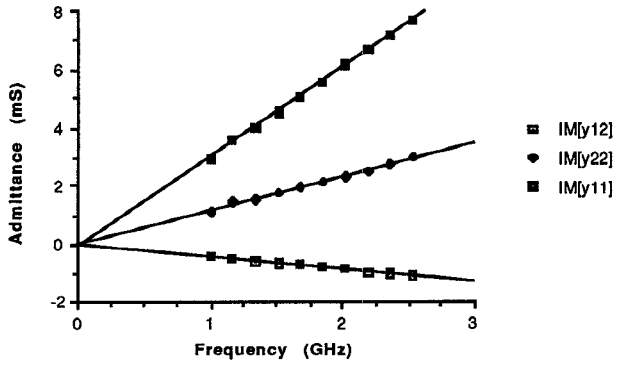

Fig. 2. Imaginary portions of eqs. (5), (6) and (8) vs. frequency with parasitic resistances de-embedded for a Triquint FET. Intrinsic device capacitances are easily extracted from the slopes of the plots.

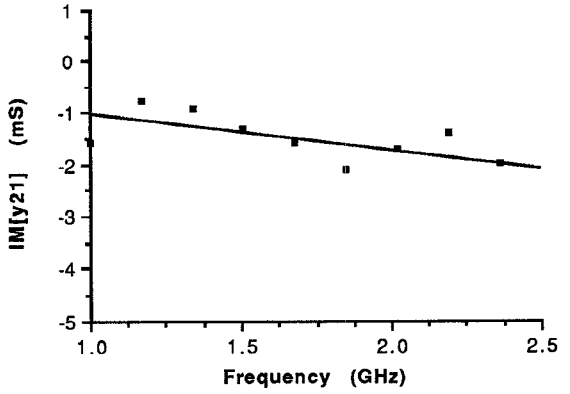

Fig. 3. Imaginary portion of eq. (7) vs. frequency with parasitic resistances de-embedded for a Triquint FET. The transit time τ can be computed from the slope of the plot once R_i, g_m, C_{gs}, and C_{gd} have been determined.

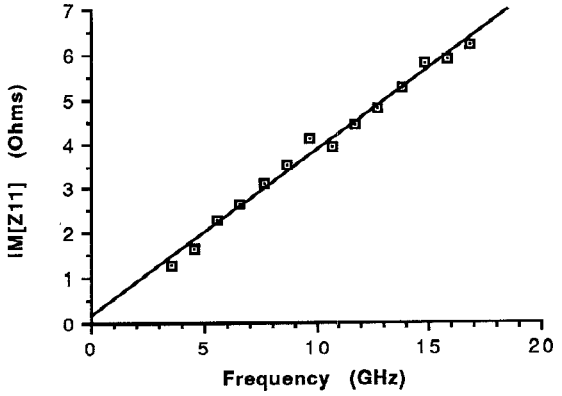

Fig. 4. Imaginary portion of ΔZ_{11} (eq. 9) vs. frequency for a Triquint FET. The inductance (L_g + L_s) is obtained from the slope of the plot.

for equation (13) were found to be W_{12} = 1 and W_{21} = 0. Hence, equation (11) is not needed in this example. The drain inductance for the device is essentially zero. The good linearity

TABLE I

Extracted Equivalent Circuit Element Values

Quantity	First Iteration	Second Iteration
C_{gd} (fF)	65.67	65.42
C_{gs}(fF)	398.3	396.5
C_{ds}(fF)	109.2	109.9
R_{ds} (Ω)	292.9	291.1
g_m (mS)	46.38	46.20
τ (ps)	1.82	1.63
L_s (pH)	0.0	3.4
L_d (pH)	0.0	0.0
L_g (pH)	0.0	59.5
E_{11}	11.2 %	0.6 %
E_{12}	3.9 %	2.3 %
E_{21}	8.3 %	4.4 %
E_{22}	2.5 %	1.7 %
E_{tot}	6.5 %	2.3%

demonstrated by the measured data illustrates the validity of the inductance extraction method. From eq. (9), the slope of the best fit line represents the inductance (L_g + L_s). The inductance values are given in the second column of Table I along with the intrinsic elements obtained after de-embedding *both the resistances and inductances.* The small change in intrinsic elements of column 1 and column 2 further demonstrate the validity of the approximation used in obtaining inductance values. The s-parameters for our model are plotted against the measured s-parameters in Figure 5.

C. Multiple Bias Extraction

Most of the large-signal models in use today have only 4 intrinsic elements which vary with bias. These are the transconductance g_m, the output conductance g_{ds}, and the gate-source and gate-drain capacitances C_{gs} and C_{gd}. All the other intrinsic elements, C_{ds}, τ and R_i are either neglected or held at some fixed value. We have found that an excellent match to s-parameters can be obtained over bias by allowing the 4 bias dependent elements to vary while constraining C_{ds}, τ and the parasitic inductances to their I_{DSS}/2 values. Shown in Figure 6 is the average error of the 4 s-parameters (1-18 GHz) as a function of drain and gate bias as computed by our extractor. These results were obtained from the same Triquint device described in section C with the non bias-dependent elements constrained to the values given in Table I. The bias dependence of g_m, g_{ds}, C_{gs} and C_{gd} is extracted in this process. This entire extraction process (25 biases) is automated by our software and takes less than 2 minutes to execute on an IBM AT machine. The match to measured s-parameters is good, and the accuracy of any large-signal model will likely be limited by the model's ability to provide a simultaneous match to the 4 bias dependent RF elements and the measured d.c. characteristics.

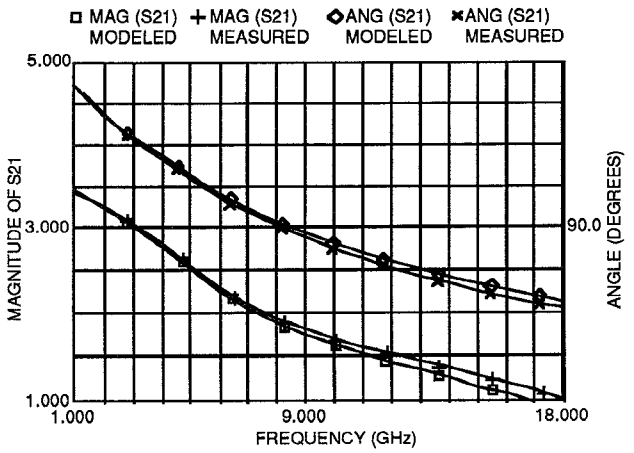

(a) Magnitude and Angle of S_{21}

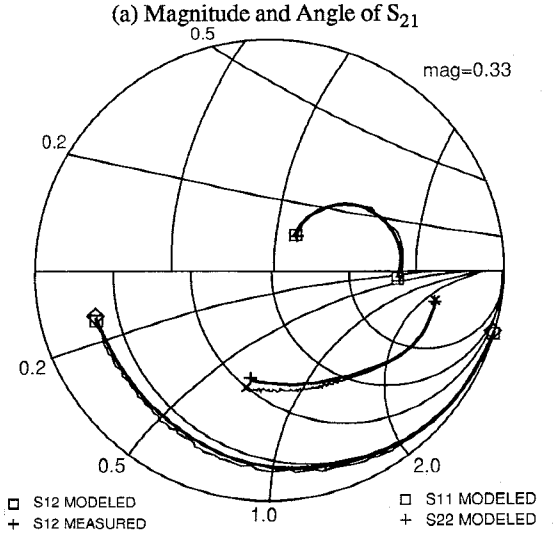

(b) S_{11}, S_{22}, and S_{12}

Fig. 5. Measured vs. modeled s-parameters from 1-18 GHz. Device is Triquint 0.5 μ by 300 μ, V_{gs} = -0.8 V, V_{ds} = 3.0 V. Element values are those in Table I, column 2.

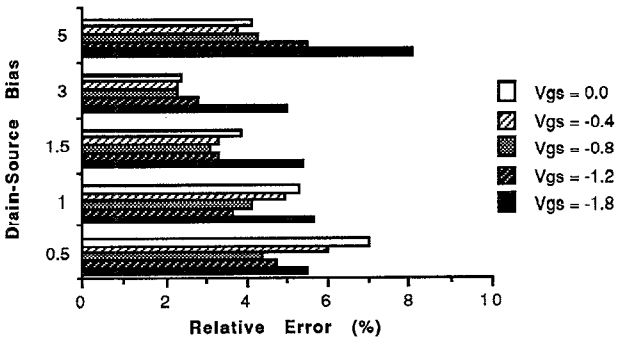

Fig. 6. Average relative s-parameter error (measured vs. modeled) computed from eq. (14) from 1-18 GHz as $(E_{11}+E_{12}+E_{21}+E_{22})/4$ over gate and drain bias variation. Parasitics, C_{ds}, and τ were constrained to their $I_{DSS}/2$ values.

IV. CONCLUSION

A simple method for extracting the intrinsic element and parasitic inductance values for a MESFET small-signal model has been outlined. After determining the parasitic resistances from d.c. measurements, the remaining elements are computed directly from a single set of measured s-parameters. The method is very fast, and its models provide an excellent match to measured s-parameters throughout the saturation region. Because the inductances are extracted at the same bias that the device is operated, any inconsistencies arising from bias variation of the inductances is eliminated.

By constraining the parasitic element values, Cds, and τ values to their 1/2 I_{DSS} values, our extractor is able to extract the bias dependence of g_m, g_{ds}, C_{gs} and C_{gd}, with a match to measured s-parameters from 1-18 GHz within approximately 5 % throughout the saturation region. This is an important result, since it is these 4 bias dependent elements which are included in most large-signal models. This bias dependent RF data along with the d.c. I-V measurements provides the starting point for the extraction of large-signal model parameters [10].

REFERENCES

[1] E.W. Strid, "Extracting more accurate FET equivalent circuits," *Monolithic Technology*, pp. 3-7, Oct. 1987.

[2] H.A. Willing, C. Rauscher, and P. deSantis, "A technique for predicting large-signal performance of a GaAs MESFET," *IEEE Trans. Microwave Theory Tech.*, vol. MTT-26, pp. 1017-1023, Dec. 1978.

[3] R. Goyal, Ed., *Monolithic Microwave Integrated Crcuit Technology and Design*, Chapter 4. Dedham, MA: Artech House, 1989.

[4] R. Vaitkus, "Uncertainty of the values of the GaAs MESFET equivalent circuit elements extracted from measured two-port scattering parameters," *Proc. IEEE/Cornell Conf. High-Speed Semiconductor Devices and Circuits*, Aug. 15-17, 1983, pp. 301-308.

[5] G. Dambrine, A. Cappy, F. Heliodore, and E. Playez, "A new method for determining the FET small-signal equivalent circuit," *IEEE Trans. Microwave Theory Tech.*, vol. MTT-36, pp. 1151-1159, July 1988.

[6] P. Ladbrooke, *MMIC Design: GaAs FETs and HEMTs*. Deham, MA: Artech House, 1989.

[7] H. Fukui, "Determination of the basic device parameters of the GaAs MESFET," *Bell Syst. Tech. J.*, vol. 58, no. 3, pp. 771-795, 1979.

[8] R.A. Minasian, "Simplified GaAs MESFET model to 10 GHz," *Electron. Lett.*, vol. 13, no. 8, pp. 549-551, 1977.

[9] M. Sango, O. Pitzalis, L. Lerner, C. McGuire, P. Wang, and W. Childs, "A GaAs MESFET large-signal model for nonlinear analysis," in *1988 IEEE MTT-S Int. Microwave Symp. Dig.* (N.Y.), May, 1988, pp. 1053-1056.

[10] M. Miller, et al., "Choosing an optimum large signal model for GaAs MESFETs and HEMTs," *1990 IEEE MTT-S Int. Microwave Symp. Dig.* (Dallas), May, 1990.